# Automatic Perceptual Color Quantization of Dermoscopic Images

Vittoria Bruni[1],Giuliana Ramella[2] and Domenico Vitulano[2]
[1]*Department of SBAI, University of Rome La Sapienza, Rome, Italy*
[2]*Institute for the Applications of Calculus, CNR, Rome, Italy*

Keywords: Color Quantization, Perception Laws, Visual Quality, Dermoscopy.

Abstract: The paper presents a novel method for color quantization (CQ) of dermoscopic images. The proposed method consists of an iterative procedure that selects image regions in a hierarchical way, according to the visual importance of their colors. Each region provides a color for the palette which is used for quantization. The method is automatic, image dependent and computationally not demanding. Preliminary results show that the mean square error of quantized dermoscopic images is competitive with existing CQ approaches.

## 1 INTRODUCTION

Color Quantization (CQ) is the process that selects and assigns a limited set of colors for representing a color image with maximum fidelity (Burger and Burge, 2009). The need of performing a CQ process frequently arises in image display (Heckbert, 1982; Weeks, 1998) and image compression (Wallace, 1991; Plataniotis and Venetsanopoulos, 2000). Moreover, CQ is considered as a prerequisite for many image processing tasks (i.e. color segmentation, color-texture analysis, content based retrieval) and it also has a wide range of applicative field. In particular, CQ plays an important role in dermoscopy since the colors of melanin, the most important chromophore in melanocytic neoplasms not visible by the naked eye, essentially depend on its localization in the skin (Braun et al., 2005; Korotkov and Garcia, 2012; Celebi et al., 2013). Even though CQ task is easy, rapid and efficient for a human observer (Rosch, 1978; Kuriki, 2004), CQ implementation is a very difficult task (NP-complete) (Braquelaire and Brun, 1997).

In the literature CQ has been widely studied and several methods have been proposed. The critical common aspect to all methods is the efficient simulation of the visual perception process that minimizes the error relative to the image quality. CQ existing methods can be classified in numerous ways on the basis of criteria taking into account different features of the CQ method at hand (Brun and Trmeau, 2002; Celebi, 2011). According to the adopted image processing technique, CQ based on clustering (Celebi et al., 2014), evolutionary approach (Hruschka et al., 2009), histogram analysis (Ramella and di Baja, 2013), neural network (Palomo and Domnguez, 2014), perceptual laws (Beghdadi et al., 2013), and so on, can be distinguished. Here we focus our attention on perception-based CQ methods since we are interested to investigate how the visual laws can be used to guide efficiently the CQ processing of dermoscopic images. Since there are several ways to include visual perception into a CQ scheme, there exists a large number of papers on this topic. At least two main sub-classes of methods can be distinguished for the this special category: the ones based on DCT/DWT transform, that are oriented to improve JPEG standard from a perceptual point of view (Battiato et al., 2001); and the ones based on visual distortion, where a visual threshold-based processing for the quantization error of quality measures is employed (Schaefer and Nolle, 2014).

In this paper, we propose to incorporate human perception into a CQ scheme by using visibility laws (Bruni et al., 2006) based on the measure of the contrast sensitivity, the luminance adaptation and the contrast masking according to the color variable perceptive context determined by the original color distribution. To this purpose we determine iteratively a hierarchical color regions partition according to their color importance at perceptive level and we compute the dominant color of the partition until a fixed number of colors is obtained. In the successive step a suitable color mapping is performed. Our perceptual-based method is automatic since perceptive thresholds are automatically tuned according to the analyzed image;

Bruni V., Ramella G. and Vitulano D..
Automatic Perceptual Color Quantization of Dermoscopic Images.
DOI: 10.5220/0005304903230330
In *Proceedings of the 10th International Conference on Computer Vision Theory and Applications* (VISAPP-2015), pages 323-330
ISBN: 978-989-758-089-5

it can be considered as context adaptable, since the resulting CQ is image-dependent. With regard to the specific domain of the images (dermoscopy), the results of this preliminary study, evaluated in terms of MSE and MAE and compared with those obtained by other authors (Celebi et al., 2013), are encouraging. The computational load required by the algorithm is very moderate and comparable to the most performing color quantization methods.

The outline of the paper is the following. Section 2 gives a detailed description of the general perceptual model. Section 3 provides a thorough description of the main steps of the whole quantization procedure. Experimental results and discussions are in Section 4 while concluding remarks are drawn in Section 5.

## 2 PERCEPTUAL MODEL

Even though the image can be composed of different colors, human eye is able to classify and detect its dominant colors after observing the image just for few milliseconds. It means that the visual mechanisms of the early vision (preattentive phase) are not completely independent on those colors that mainly characterize the observed scene (image). In the case of dermoscopic images, the object of interest is well defined since the context of the images is limited (usually image background is the skin) and then anomalies of the skin attract human attention at the first glance — some examples are shown in Fig. 1. Based on these considerations, the problem of CQ in dermoscopic images can be viewed in the more general context of the detection of local image anomalies. In fact, as several neurological studies show, if on the one hand human eye is used to recognize those regions in the image with which it is very familiar; on the other hand, it is instinctively attracted by the most unnatural parts of the image, probably due to safety instincts (i.e. to check if there are dangers/unnatural components in the scene) (Monte et al., 2005; Frazor and Geisler, 2006; Moorthy and Bovik, 2009). That is why in this paper we aim at modelling the dermoscopic image as an image with a given distortion, namely skin mole (melanoma), and we want to detect and characterize it by means of a hierachical detection of those image regions that attract human attention at the first glance. To this aim we consider the defect detection method in (Bruni et al., 2006; Bruni et al., 2013) and we adapt it to the case of dermoscopic images. The main features of this model are:

- to project the analysed image into a new space that is able to better reproduce image components in a way that is consistent with their visual perception at the first glance: for example, the objects that attract first human attention are the brighter parts in the projected image. The projection space has to depend on the kind of image and the characteristic of the distortion;
- to define the level of resolution that reproduces the perceived image information: human eye is not sensitive to fine textures in the preattentive phase; that is why, usually textured regions are perceived as uniform regions having constant color. The level of resolution is used for the characterization of a low pass filter to apply to the projected image;
- to define a detection operator whose goal is to detect those regions in the projected and filtered image that correspond to the ones that attract more eye attention at the first glance. Since, the projection space is selected as the one where image anomalies become the brighter part of the image, a thresholding operator is used for detection and the threshold is automatically selected by measuring the local and global visual image contrast.

This general model has some nice features. It is completely automatic and does not require user's intervention in parameters setting; it is simple since it is based on simple operations like linear filtering, contrast evaluation and thresholding operations; it is not computationally demanding and it is easy to implement making it useful for real time applications.

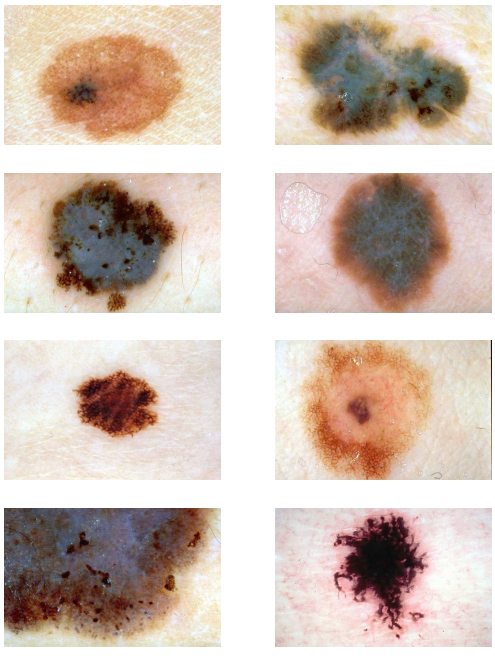

Figure 1: Eight dermoscopic images. From left to right, top to bottom: Acl285, Nbl034, Nbl063, Nml012, Ael484, Fel096, Nml024 and Newl012 (Argenziano et al., 2002).

# 3 PERCEPTUAL COLOR QUANTIZATION

The selection of the projection operator to apply to the original image, as explained in the previous section, has to take into account the class of images and the type of application we are dealing with. This step tries to simulate the human visual system that reacts in the presence of different colored objects in the scene. In the specific case of dermoscopic images we have to consider both color perception and the presence of skin anomalies. On the other hand, in this paper we do not want to use too complicated models in order to limit the computational effort of the whole procedure. That is why the luminance component of the YIQ color space (Gonzalez and Woods, 2002) has been considered. The YIQ system takes advantage of human color-response characteristics. In particular, it is based on the sensitiveness to changes in the orange-blue (I) range than in the purple-green range (Q) - therefore less bandwidth is required for Q than for I. In addition, Y (that represents the luminance component and preserves the 90% of the whole image information (Winkler, 2005)) is the one used for black and white television and it is a weighted average of red, green and blue components. The weights reflect the fact that human eye is more sensitive to green than red, but is more sensitive to red than blue; that is why the weights in the average are about .3, .6 and .1 respectively for red, green and blue color components.

Finally, since melanoma are in general of dark colors with respect to the skin, and since we are interested in better distinguishing those colors that characterize it for clinical purposes, the negative of $Y$ component has been considered. In this way, skin anomalies become the brighter parts of this component. An example is shown in Fig. 2.

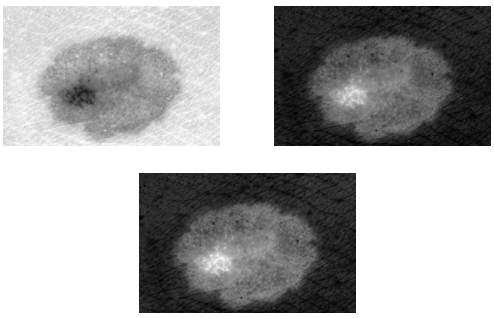

Figure 2: Acl285 test image. From left to right, top to bottom: Image luminance component $Y$; negative of the luminance $Y$; filtered version of $\bar{Y}$ at the optimal resolution $\bar{r}$ ($1^{st}$ level of a db2 wavelet decomposition has been automatically selected).

As mentioned above, in the preattentive phase, human eye acts as a low pass filter since it is not interested in the detection of image details in this phase. As a result non-homogeneous colored image regions are usually perceived at the first glance as uniform areas. For the selection of this "visual resolution" (and then the order of the low pass filter to be applied to the image), the same arguments and methods given in (Bruni et al., 2006; Bruni et al., 2013) have been used. The "visual resolution" must be a good trade off between the enhancement of the degraded region and the preservation of their geometrical shape and color features. Perception rules are employed also for the selection of this resolution $\bar{r}$, that is automatically selected by computing the contrast between two successive low-pass filtered versions of the detection space. A moving average filter $\phi_r$ of order $r$ can be then used to smooth the negative of the $Y$ component, namely $\bar{Y}$. The rationale is that the best level of resolution $\bar{r}$ is that which measures the minimum perceivable contrast, i.e. 0.02 (Winkler, 2005), between two successive blurred images, i.e.

$$\bar{r} = argmin_{r\in\mathbf{N}}\{C(r) \leq 0.02\}. \quad (1)$$

where

$$C(r) = \int_{\Omega} \frac{|\bar{Y} * \phi_r(x,y) - \bar{Y} * \phi_{r-1}(x,y)|}{|\Omega|\,(\bar{Y} * \phi_r(x,y))} dxdy, \quad (2)$$

is the definition of visual contrast given by Peli (Winkler, 2005), $\Omega$ is the image domain and $|\Omega|$ is its size. It is worth observing that $\phi_r$ is a low pass filter; hence the numerator of the integrand function in eq. (2) is a sort of derivative of $\bar{Y}$, while $\bar{Y} * \phi_r$ is its local mean.

Fig. 3 depicts a typical behaviour of the contrast curve $C(r)$ versus the level of resolution $r$: it is a decreasing function and the optimal point $\bar{r}$ coincides with the maximum inflection of the curve. The value of $\bar{r}$ can be associated to a precise scale level $J$ in a pyramidal decomposition (for instance a dyadic wavelet decomposition) by means of the equation $J = \lceil \log_2 \left(\frac{\bar{r}}{H}\right) \rceil$, where $H$ is the length of the filter associated to the adopted wavelet (Mallat, 1998), see (Bruni et al., 2006) for details. In our experiments the low pass filter associated to the Daubechies wavelet with 2 vanishing moments (Mallat, 1998) has been adopted since it has minimum support and reasonable regularity that are well adapted to the analysed images. Let $\bar{Y}_r$ be the low pass filtered version of $\bar{Y}$. As it can be observed in Fig. 2, skin anomalies are the brighter objects in $\bar{Y}_r$.

## 3.1 Selection of Dominant Colors

The objective of this section is to iteratively separate $\bar{Y}_r$ foreground (skin anomalies) and background. The

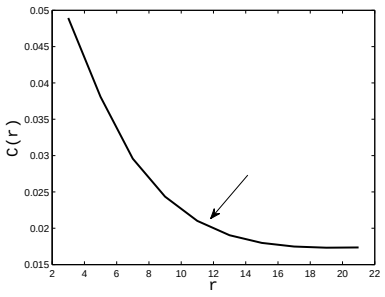


Figure 3: Contrast $C(r)$, as in eq. (2), versus the resolution $r$. The arrow indicates the optimal resolution $\overline{r}$.

goal is to iteratively detect image regions according to their visual importance (from the most to the less important in the pre-attentive vision process). The number of iterations is represented by the number of colors $K$ to be used for image quantization; $K$ is considered as an input known value. In particular, regions of interest in $\tilde{Y}_r$ are selected using a threshold value that has to correspond to the point of maximum visibility of the foreground with respect to its background. To this aim, a suitable distortion based on the image visual contrast is defined.

Let $M$ be the mean value of $\overline{Y}_r$, that measures its global background; let us define a reference image $\overline{Y}_M$ as follows

$$\overline{Y}_M(x,y) = \begin{cases} \overline{Y}_r(x,y) & \text{if } \overline{Y}_r(x,y) \geq M \\ M & \text{otherwise;} \end{cases} \quad (3)$$

and let $\mathcal{T}(\overline{Y}_M, T)$ be the clipping operator, i.e.

$$\mathcal{T}(\overline{Y}_M, T)(x,y) = \begin{cases} \overline{Y}_M(x,y) & \text{if } \overline{Y}_M(x,y) \leq T \\ T & \text{otherwise.} \end{cases} \quad (4)$$

The goal is to select a suitable value for $T$ (namely $\overline{T}$) that is able to separate $\overline{Y}_M$ foreground (the brightest regions) from the rest of the image. In particular, $\overline{T}$ will be the one that maximizes a visual distortion $D$ that depends on both local and global image contrast, as explained in the following.

**Definition 1.** Let $\Omega_T = \{(x,y) \in \Omega : \overline{Y}_M(x,y) > T\}$ be the set of pixels whose $\overline{Y}_M$ value over-exceeds the threshold value $T$. Let $D_1$ and $D_2$ be defined as

$$D_1(x,y) = \frac{\overline{Y}_M(x,y) - \mathcal{T}(\overline{Y}_M, T)(x,y)}{M}$$

$$D_2(x,y) = \frac{\overline{Y}_M(x,y)|M_T - M|}{M_T M},$$

with $M_T$ the average value of $\mathcal{T}(\overline{Y}_M, T)$ in $\Omega - \Omega_T$, then the *visual distortion* for the set $\Omega_T$ is defined as

$$D(\Omega_T) = \frac{1}{|\Omega_T|} \sum_{(x,y)\in\Omega_T} D_1(x,y) D_2(x,y). \quad (5)$$

The distortion $D$ describes the interaction between image background and foreground. $D_1(x,y)$ measures the contrast variation of a changing object with respect to a fixed background: the contrast is measured through the Weber's law, the changing object is a region of $\overline{Y}_M$ before and after clipping, while the fixed background is given by $M$. Hence, $D_1$ evaluates how an object changes its perception if it is substituted for the threshold value $T$. It is worth outlining that: *i)* $D_1(x,y) = 0 \quad \forall\,(x,y) \in \Omega - \Omega_T$; *ii)* the value of $D_1$ in $\Omega_T$ is an increasing function for decreasing threshold values (increasing $|\Omega_T|$). In particular, $D_1(\Omega_T)$ grows quickly for higher thresholds since clipping involves less uniform regions with small area; on the contrary, the growing law changes as the threshold value decreases, since the clipping selects many points whose values are closer to the background.

$D_2$ measures the contrast variation of the same object of $\overline{Y}_M$ over different backgrounds — $M_T$ is the background of the image after the clipping operation and it decreases toward $M$ as $T$ decreases. $D_2$ is the product of two different components: the former, $\frac{\overline{Y}_M}{M_T}$, is a growing function as $M_T$ decreases. The latter, $\frac{|M_T - M|}{M}$, is a decreasing function converging to zero for smaller threshold values. Hence, $D_2$ reveals a convex shape. In fact, the term $\frac{|M_T - M|}{M}$ gives a minor contribution in the first part, since the clipping operator involves few pixels and then $M_T$ does not change significantly. On the contrary, in the second part $M_T$ approaches $M$ faster, as more points close to the background are selected, and then $D_2$ approaches zero.

The visual distortion $D$ combines $D_1$ and $D_2$ using a multiplicative model, that is the conventional way of combining contrast based measures. Since $D_1$ increases while $D_2$ decreases, the optimal separation point is the equilibrium point of the product of the two measures. Then, the optimal detection threshold $\overline{T}$ is the one that realizes the maximum value of $D$ (see Fig. 4) and provides the frontier between image foreground and background. From that point on, pixels of the background are selected by the clipping operator, confusing the most visual attractive part of image with the remaining part. The most visually important region $\Omega_1$ in $\overline{Y}_r$ is then defined as $\Omega_1 = \{(x,y) \in \Omega : Y_r(x,y) \geq \overline{T}\}$.

The mean value of the colors (in the RGB color space) of points belonging to $\Omega_1$ is considered as the dominant color of the region and it is set to the first value $\mathbf{c}_1$ of the color palette to be used in the quantization step. By excluding from the image the selected region $\Omega_1$, the procedure can be reapplied to the remaining part of the image $(\Omega - \Omega_1)$ in order to select a number of representative regions from which to extract the dominant colors to add to the desired color

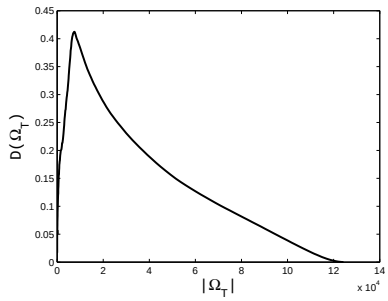


Figure 4: Distortion curve $D(\Omega_T)$ versus the size of $\Omega_T$.

palette. As a result, the detection algorithm is iterated $K$ times, with $K$ the number of desired colors in the palette. In order to adapt the algorithm to the number of desired colors, the value $M$ in eq. (3) is differently defined and computed at each iteration. In fact, the detection algorithm can be less sensitive to some details as $K$ decreases; while it is the opposite as $K$ increases. That is why, the value $M$, that represents the image background, is defined as a correction of the average value of the image to be analysed. The correction term is defined as $1-k\frac{|M_{av}-Mo|}{M_{av}}$, where $k$ is the $k-th$ region we are going to select while $M_{av}$ and $Mo$ respectively are the average value and the most frequent value of $\overline{Y}_r$.

## 3.2 Algorithm

1. Convert the original RGB image to the luminance component $Y$.
2. Find the best level of resolution $\overline{r}$ via eq. (1) and compute the blurred negative of $Y$, i.e. $\overline{Y}_r$.
3. Compute the mean value $M_{av}$ and the mode $Mo$ of $\overline{Y}_r$ and repeat the following steps $K$ times (for $k = 1,2,\ldots,K$)
   - Compute the mean value of $\overline{Y}_r$; set $M = M\left(1-k\frac{|M_{av}-Mo|}{M_{av}}\right)$ and evaluate eq. (3).
   - For each integer $T \in [M,255]$, in decreasing order, evaluate $D(\Omega_T)$.
   - Extract the optimal $\overline{T}$ as the maximum point of the curve $(|\Omega_T|, D(\Omega_T))$.
   - Extract the binary mask: $\Omega_k(x,y) = \begin{cases} 1 & \text{if } \overline{Y}_r(x,y) \geq \overline{T} \\ 0 & \text{otherwise.} \end{cases}$
   - Compute the average color $\mathbf{c}_k$ of image pixels such that $\Omega_k(x,y) = 1$ and put it in the palette.
   - Set $\Omega = \Omega - \Omega_k$ and $\overline{Y}_r = \overline{Y}_r(\Omega)$
4. Assign to each pixel in the original image the closest color in the selected color palette $\{\mathbf{c}_1, \mathbf{c}_2, \ldots, \mathbf{c}_K,\}$ and let $I_Q$ the quantized image.

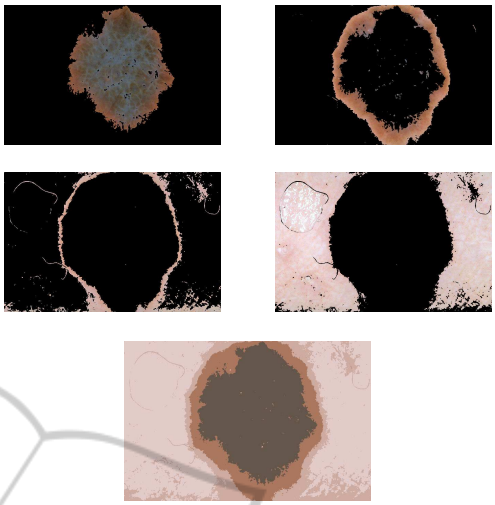

Figure 5: Test Image Nml012. From left to right, top to bottom: regions $\Omega_1, \Omega_2, \Omega_3, \Omega_4$ selected by the proposed algorithm and the quantized image ($K = 4$).



# 4 EXPERIMENTAL RESULTS

The proposed method has been tested on several images extracted from different dermoscopy databases. The results presented in this section concern eight test images contained in the database included in (Argenziano et al., 2002) in order to provide fair comparative studies with existing methods.

Accounting for the medical interest for the characterization of melanoma according to its different colors, the results we are going to present in this section concern the selection of very few colors from the original image to be used in the definition of the new color palette, i.e., $K = 4,6,8$, that is fixed by the user. The quantization results will be measured in terms of Mean Square Error (MSE) between the original and the quantized image, and also in terms of Mean Absolute Error (MAE). The evaluation of the results will be made by means of comparisons with some well known methods for CQ, especially the ones that have been used in the processing of dermoscopic images. To this aim we have considered the work in (Celebi et al., 2013) (WSM), since it is very recent and provides very impressive results on dermoscopic images. In addition, it provides several comparative studies with existing CQ algorithms. WSM consists of an optimization of the classical K-means clustering procedure from both computational and faithfulness of the results points of view. In particular, it refines the inizialization step of the K-means algorithm and optimizes its implementation. In addition, we compare the proposed method with the Median-Cut (MC)

Table 1: MSE and MAE (in the brackets) results on some test dermoscopic images achieved by the methods in (Heckbert, 1982; Wu, 1991; Cheng and Yang, 2001; Celebi, 2009; Celebi et al., 2013) and the proposed one for a different number $K$ of colors in the palette.

| Method | $K$ | *Acl285* | *Nbl034* | *Nbl063* | *Nml012* | *Ael484* | *Fel096* | *Nml024* | *Newl012* |
|---|---|---|---|---|---|---|---|---|---|
| | 4 | 759.1 (35.7) | 1177.3 (47.5) | 1610.4 (54.9) | 1400.2 (46.3) | 625.9 (31.6) | 945.4 (41.3) | 1761.6 (56.2) | 770.5 (36.8) |
| MC | 6 | 639.1 (33.2) | 939.8 (41.9) | 892.2 (41.8) | 520.0 (31.2) | 524.6 (29.7) | 787.5 (38.2) | 1016.2 (43.0) | 655.8 (34.8) |
| | 8 | 526.1 (30.2) | 761.7 (37.5) | 791.0 (39.2) | 418.4 (27.8) | 379.5 (26.0) | 762.8 (37.6) | 960.7 (41.6) | 528.9 (31.9) |
| | 4 | 823.9.4 (37.9) | 1325.0 (50.6) | 1283.6 (50.3) | 1331.8 (46.6) | 684.2 (34.8) | 1027.1 (43.2) | 1735.5 (56.3) | 852.7 (39.9) |
| CY | 6 | 433.9.9 (26.3) | 777.6 (37.9) | 708.1 (36.5) | 479.9 (29.6) | 410.9 (27.8) | 572.3 (31.1) | 956.7 (42.2) | 567.5 (31.0) |
| | 8 | 329.5.0 (22.8) | 533.1 (30.9) | 486.5 (29.7) | 371.0 (25.5) | 234.9 (19.6) | 424.5 (27.8) | 561.0 (32.8) | 381.0 (26.4) |
| | 4 | 786.7 (36.2) | 1249.0 (48.1) | 1086.0 (44.0) | 922.6 (38.1) | 598.6 (30.3) | 1182.1 (44.0) | 1444.3 (52.6) | 776.1 (37.2) |
| WU | 6 | 477.6 (27.3) | 779.9 (37.1) | 751.0 (36.3) | 458.0 (27.4) | 295.3 (20.5) | 540.4 (30.4) | 825.2 (38.8) | 477.7 (28.5) |
| | 8 | 283.7 (22.0) | 628.2 (33.1) | 509.9 (28.6) | 306.8 (22.7) | 228.6 (17.9) | 380.1 (24.5) | 592.9 (32.4) | 354.0 (24.1) |
| | 4 | 718.8 (33.5) | 1242.5 (49.5) | 1085.8 (44.9) | 1133.4 (45.6) | 1070.9 (30.6) | 1329.8 (40.1) | 1443.2 (53.0) | 1000.4 (35.8) |
| ADU | 6 | 406.7 (24.6) | 648.3 (33.6) | 674.9 (34.7) | 466.7 (28.2) | 685.3 (24.3) | 491.9 (29.4) | 789.0 (38.5) | 409.2 (26.3) |
| | 8 | 297.1 (21.3) | 476.3 29.0) | 457.3 (27.3) | 292.1 (22.0) | 240.4 (16.4) | 334.2 (23.1) | 587.5 (32.9) | 310.2 (22.2) |
| | 4 | 714.6 (**33.0**) | 1147.0 (**46.5**) | 1062.2 (**43.7**) | 789.1 (37.1) | 522.8 (29.1) | 884.4 (40.3) | **1316.6** (**50.5**) | 726.6 (35.6) |
| WSM | 6 | 359.8 (24.5) | **637.0** (**33.6**) | 726.2 (35.8) | 412.8 (26.3) | 256.5 (19.7) | 436.8 (27.1) | **763.7** (**37.2**) | **393.8** (**26.4**) |
| | 8 | 234.5 (19.9) | **458.9** (**28.4**) | **405.4** (**26.8**) | **274.3** (**21.5**) | **173.5** (15.9) | 313.1 (22.5) | **550.7** (**31.6**) | **281.8** (**22.4**) |
| | 4 | **658.4** (33.7) | **1126.1** (48.9) | **986.7** (44.1) | **546.9** (**31.4**) | **415.1** (**26.2**) | **786.9** (**36.2**) | 1613.8 (53.0) | **711.2** (**35.2**) |
| PCQ | 6 | **319.9** (**23.5**) | 640.2 (34.2) | **623.0** (**32.2**) | **349.9** (**24.1**) | **253.9** (**17.3**) | **420.7** (**26.4**) | 765.3 (37.6) | 508.2 (26.8) |
| | 8 | **199.0** (**18.1**) | 516.7 (29.4) | 577.5 (29.5) | 292.8 (21.6) | 226.4 (**15.2**) | **302.2** (**21.0**) | 565.5 (32.3) | 431.3 (23.4) |

(Heckbert, 1982) and its modifications in (Cheng and Yang, 2001) CY and (Wu, 1991) WU. Similarly to the proposed method, all of them are based on a recursive optimization of color histogram but they use different criteria and measures (respectively variances and directional distances from the mean) that do not explicitely depend on visual perception rules. The results have also been compared with the Adaptive Distributing Units (ADU)(Celebi, 2009) that is a learning clustering algorithm. Even though some of these methods are not recent, they perform quite well on dermoscopic images.

Table 1 gives MSE and MAE results provided by the selected methods and the proposed one, indicated with PCQ (Perceptual Color Quantization), on the same test images and for different number of desired colors $K$; the best results are in bold. As it can be observed, the proposed method is able to outperfom its competitors in most cases. In particular, it is able to greatly improve WSM results when the desired number $K$ of colors in the palette is small, while it shows comparable results when $K$ increases. This is very interesting as the challenge of any information coding framework is to get better performance at very low bit rates. It is worth noting that the proposed method does not use any refinement of both the final and the partial results in the definition of the color palette. As it can be observed in Figs. 5 and 6, the quantized image reflects the color content and also the nature of the image content, giving a consistent segmentation of skin anomalies and skin itself. Figure 5 also depicts all the intermediate steps of the detection procedure and shows the regions from which the dominant color is extracted.

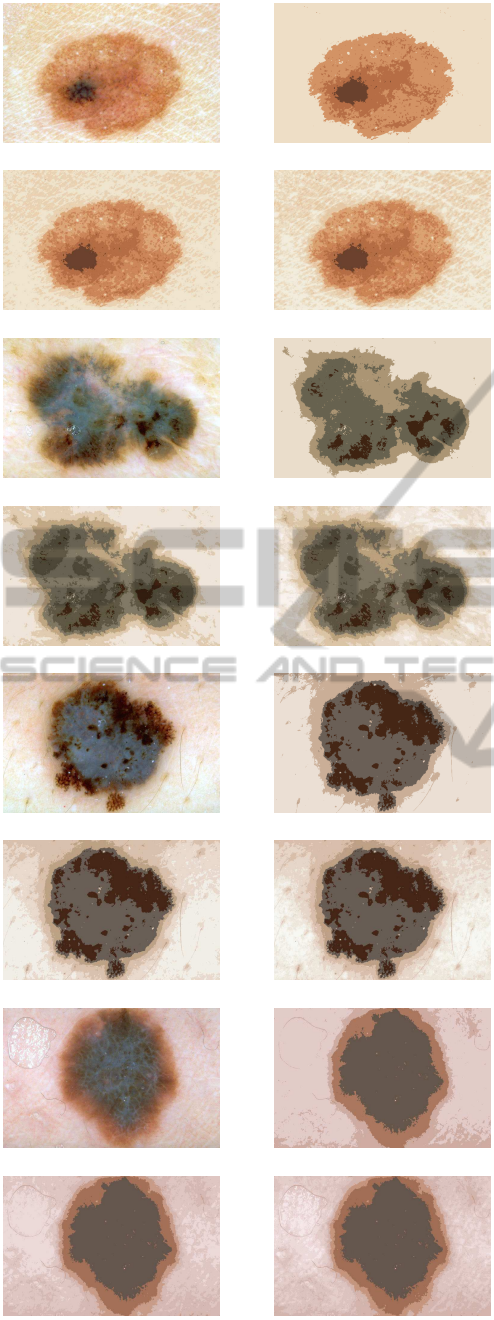

Figure 6: For each selected test image: original image and its quantized version for different number of desired colors (from top to bottom: $K = 4, 6, 8$).

It is worth stressing that the proposed method is completely automatic, since it is able to adapt to the analysed image thanks to the consistent use of perception rules in the whole procedure (from the projection space to the selection of the best threshold for separating image background and foreground). It is also competitive from the computational point of view. In fact, as it is evident from the Algorithm, the method uses simple linear operations or comparisons. In particular, the complexity of the method depends on the number of colors $K$ in the final palette as well as on the number of gray levels $N'$ in the projected and filtered luminance component (i.e. less than 256). Hence, the complexity of each iteration of the method (step 3 of the Algorithm) is $O(N')$, and then the complexity for the selection of the colors in the final palette is $O(KN')$. The additional cost required by the computation of $\overline{Y}_r$ is proportional to the image size and does not depend on the desired number of colors $K$, making the method competitive even with respect the computational point of view.

## 5 CONCLUSIONS

The paper has presented a new method for CQ of dermoscopic images that is based on the use of some visual perception laws at the early stage. The goal of the method is to detect in a hierarchical way those regions in the image that attract human attention at the first glance, and to derive from each of them a dominant color to use in the successive quantization step. To this aim the color image is transformed in a gray-level image at a given resolution where the brighter parts represent the regions that attract human attention at the first glance; then, a proper visual distortion measure is used for iteratively selecting adaptive thresholds that separate regions having different visual importance. Presented results are encouraging since the method is completely automatic, image dependent and requires low computing time, resulting competitive with existing approaches. Future research will be oriented to the extension of the method to a wider class of images. This extension would require the choice of a projection space that is more consistent with the way colors are perceived by human eye, and a finer extraction of the dominant color in each selected region.

## ACKNOWLEDGEMENTS

The Authors would like to thank Prof. Celebi for having encouraged their research in color quantization of dermoscopic images.

## REFERENCES

Argenziano, G., Soyer, H., and Giorgi, V. D. (2002). *Dermoscopy:a tutorial*. EDRA Medical Publishing and

New Media, +cd edition.

Battiato, S., Mancuso, M., Bosco, A., and Guarnera, M. (2001). Psychovisual and statistical optimization of quantization tables for dct compression engines. In *Proc. 11th Int. Conf. Image Analysis and Processing*.

Beghdadi, A., Larabi, M., Bouzerdoum, A., and K.M. Iftekharuddin, K. M. (2013). A survey of perceptual image processing methods. In *Signal Processing: Image Communication, 28, 811-831*.

Braquelaire, J. and Brun, L. (1997). Comparison and optimization of methods of color image quantization. In *IEEE Trans.on Image Processing, 6 1048-052*.

Braun, R. P., Rabinovitz, H., Oliviero, M., Kopf, A., and Saurat, J. (2005). Dermoscopy of pigmented skin lesions. In *Journal of the American Academy of Dermatology, 52 (1), 109-121*.

Brun, L. and Trmeau, A. (2002). Digital color imaging handbook, chapter 9: Color quantization. In *Electrical and Applied Signal Processing*. CRC Press.

Bruni, V., Crawford, A., Kokaram, A., and Vitulano, D. (2013). Semi-transparent blotches removal from sepia images exploiting visibility laws. In *Signal Image and Video Processing, 7(1), 11-26*.

Bruni, V., Crawford, A., and Vitulano, D. (2006). Visibility based detection of complicated objects: a case study. In *Proc. of IEE CVMP 06*.

Burger, W. and Burge, M. (2009). *Principles of Digital Image Processing*. Undergraduate Topics in Computer Science, Springer-Verlag.

Celebi, M. (2009). An effective color quantization method based on the competitive learning paradigm. In *Proc. of Int. Conf. on Image Proc., Computer Vision and Pattern Rec.*

Celebi, M., Wen, Q., Hwang, S., and Schaefer, G. (2013). Color quantization of dermoscopy images using the k-means clustering algorithm. In *Color Medical Image Analysis, 87-107*. Celebi, M. E., Schaefer, G. Eds., Lecture Notes in Computational Vision and Biomechanics, 6, Springer.

Celebi, M. E. (2011). Improving the performance of k-means for color quantization. In *Image and Vision Computing 29, 260-271*.

Celebi, M. E., Hwang, S., and Wen, Q. (2014). Color quantization using the adaptive distributing units algorithm. In *Imaging Science Journal 62(2), 80-91*.

Cheng, S. and Yang, C. (2001). Fast and novel technique for color quantization using reduction of color space dimensionality. In *Pattern Recognition Letters, 22(8):845-856*. Elsevier.

Frazor, R. and Geisler, W. (2006). Local luminance and contrast in natural in natural images, 46. In *Vision Research*.

Gonzalez, R. C. and Woods, R. E. (2002). *Digital Image Processing*. Prentice Hall, 2nd edition.

Heckbert, P. (1982). Color image quantization for frame buffer display. In *Proc. ACM SIGGRAPH '82 16(3), 297-307*.

Hruschka, E., Campello, R., Leon, A. F. F. P., and de Carvalho, A. (2009). A survey of evolutionary algorithms for clustering. In *IEEE Trans. on Systems, Man, and Cybernetics, Part C: Applications and Reviews VOL. 39, 2, pp. 133-155*.

Korotkov, K. and Garcia, R. (2012). Computerized analysis of pigmented skin lesions: A review. In *Artificial Intelligence in Medicine, 56, 69-90*.

Kuriki, I. (2004). Testing the possibility of average-color perception from multi-colored patterns. In *Optical Review, 11 (4), 249-257*.

Mallat, S. (1998). *A wavelet tour of signal processing*. Academic Press.

Monte, V., Frazor, R., Bonin, V., Geisler, W., and Corandin, M. (2005). Independence of luminance and contrast in natural scenes and in the early visual system 8(12). In *Nature Neuroscience*.

Moorthy, A. and Bovik, A. (2009). Visual importance pooling for image quality assessment. In *IEEE Journal on Special Topics in Sig. Proc., 3(2)*.

Palomo, E. and Domnguez, E. (2014). Hierarchical color quantization based on self-organization. In *Journal of Mathematical Imaging and Vision, 49,1-19*.

Plataniotis, K. and Venetsanopoulos, N. (2000). Color image processing and applications. In *Communications of the ACM, 34, 30-44*.

Ramella, G. and di Baja, G. S. (2013). A new technique for color quantization based on histogram analysis and clustering. In *International Journal Pattern Recognition and Artificial Intelligence, 27 (3)*.

Rosch, E. (1978). Cognition and categorization, principles of categorization. In *Rosch, E., Lloyd, B.B. Ed., Erlbaum, Hillsdale*.

Schaefer, G. and Nolle, L. (2014). A hybrid color quantization algorithm incorporating a human visual perception model. In *Computational Intelligence*.

Wallace, G. (1991). The jpeg still picture compression standard. In *Communications of the ACM, 34, 30-44*.

Weeks, A. R. (1998). Fundamentals of electronic image processing. In *SPIE-The International Society for Optical Engineering, Bellingham, Washington USA*.

Winkler, S. (2005). *Digital Video Quality, Vision Models and Metrics*. Wiley.

Wu, X. (1991). Efficient statistical computations for optimal color quantization. In *Graphics gems*. Academic Press.